# Long-Range Targeted Manipulation of the *Drosophila* Genome by Site-Specific Integration and Recombinational Resolution

**Natalia Wesolowska*,† and Yikang S. Rong*,[1]**

*Laboratory of Biochemistry and Molecular Biology, National Cancer Institute, National Institutes of Health, Bethesda, Maryland 20892, and †National Institutes of Health Graduate Partnership Program with The Johns Hopkins University, Bethesda, Maryland 20892

**ABSTRACT** Significant advances in genomics underscore the importance of targeted mutagenesis for gene function analysis. Here we have developed a scheme for long-range targeted manipulation of genes in the *Drosophila* genome. Utilizing an *attP* attachment site for the phiC31 integrase previously targeted to the *nbs* gene, we integrated an 80-kb genomic fragment at its endogenous locus to generate a tandem duplication of the region. We achieved reduction to a single copy by inducing recombination via a site-specific DNA break. We report that, despite the large size of the DNA fragment, both plasmid integration and duplication reduction can be accomplished efficiently. Importantly, the integrating genomic fragment can serve as a venue for introducing targeted modifications to the entire region. We successfully introduced a new attachment site 70 kb from the existing *attP* using this two-step scheme, making a new region susceptible to targeted mutagenesis. By experimenting with different placements of the future DNA break site in the integrating vector, we established a vector configuration that facilitates the recovery of desired modifications. We also show that reduction events can occur efficiently through unequal meiotic crossing over between the large duplications. Based on our results, we suggest that a collection of 1200 lines with attachment sites inserted every 140 kb throughout the genome would render all *Drosophila* genes amenable to targeted mutagenesis. Excitingly, all of the components involved are likely functional in other eukaryotes, making our scheme for long-range targeted manipulation readily applicable to other systems.

*DROSOPHILA melanogaster* is an excellent organism for the genetic analysis of cellular and developmental processes. For the past two decades, methods of gene targeting by homologous recombination have facilitated the engineering of crafted mutations (Gloor *et al.* 1991; Rong and Golic 2000; Rong *et al.* 2002; Gong and Golic 2003). The wealth of information provided by bioinformatic analyses has further aided geneticists in the design of mutations. Gene targeting in flies, however, is quite labor intensive, discouraging its use in systematic mutagenesis, which involves more than one targeted allele, although success stories have revealed the benefits of such approaches (Gronke *et al.* 2010; Spitzweck *et al.* 2010).


doi: 10.1534/genetics.112.145631
Manuscript received September 4, 2012; accepted for publication October 25, 2012
Supporting information is available online at http://www.genetics.org/content/early/2012/11/06/genetics.112.145631/suppl/DC1.
[1]Corresponding author: NIH, Bldg. 37, Room 6056, 37 Convent Dr., Bethesda, MD 20892. E-mail: rongy@mail.nih.gov

Recently, several laboratories have demonstrated that, by combining homologous recombination with the efficient phiC31-mediated site-specific recombination method, the need for repetitive gene targeting of individual alleles to the endogenous locus can be eliminated (Gao *et al.* 2008; Huang *et al.* 2009; Weng *et al.* 2009; Iampietro *et al.* 2010). We developed the site-specific integrase-mediated repeated targeting (SIRT) method, in which an *attP* attachment site for phiC31 integrase is first targeted to the genome in the proximity of the locus of interest using gene targeting by homologous recombination. Further modifications are carried out by integration of a plasmid that carries the modified locus and the "partner" attachment site *attB*. Recombination between chromosomal *attP* and plasmid-born *attB* is irreversible and highly efficient in fly embryos expressing phiC31 (Groth *et al.* 2004; Bischof *et al.* 2007). Integration of the plasmid leads to duplication of the chromosomal locus, which is subsequently reduced to one copy by repair of an induced DNA double-strand break (Rong *et al.* 2002; Gao *et al.* 2008).

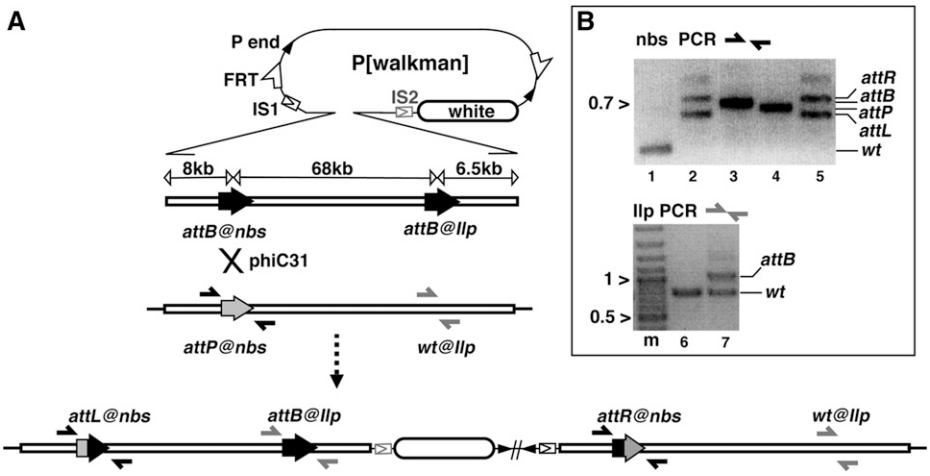


**Figure 1** Generating an 80-kb duplication by site-specific integration. (A) Integration schematic. At the top is the pWalkman vector built on the pP[acman] backbone, which contains *P*-element ends (solid arrowheads), a *white* maker (open oval), *FRT* sites (half-arrows), and an I-*Sce*I cut site (IS1 in construct pWalkman{nbs-llp} IS1 and IS2 in pWalkman{nbs-llp} IS2). Below the pWalkman vector is the 82-kb *nbs-llp* insert, which contains two *attB* sites (solid arrows), one at each locus, separated by 68 kb. Below the 82-kb insert is the chromosomal region with an *attP* (shaded arrow) targeted to *nbs*. Note that the chromosomal region of *llp* does not contain any *att* site (*wt*). The positions for two sets of PCR primers (solid and shaded half arrows) used in B are indicated. A phiC31-mediated recombination ("X") between *attP* and *attB* at *nbs* gives rise to the duplication depicted at the bottom. Only the integration of pWalkman{nbs-llp}IS1 is shown. The *FRT*s are not shown but are in close proximity to the *P*-element ends. (B) Representative results for diagnostic PCR tests. Marker size in kilobases is indicated to the left of the gel images. (Top) PCR analyses with *nbs* primers. The PCR templates are the following: lane 1, a wild-type line without any attachment site; lane 2, a duplication line from previous plasmid integration at *attP@nbs*; lane 3, plasmid DNA of pWalkman(nbs-llp)IS1; lane 4, the *attP@nbs* starting line; and lane 5, an integration line with the 80-kb duplication. (Bottom) Results of PCR analyses with *llp* primers. Lane "m" contains the marker. The PCR templates are the following: lane 6, a wild-type line, and lane 7, an integration line from this study.

One versatile aspect of SIRT not shared by traditional gene-targeting methods is that a particular *attP* site can be used to modify not only one's gene of interest, but all of the genes in its vicinity. In theory, the range amenable to SIRT manipulation from an *attP* insertion is limited only by the size of the genomic clone in the *attB*-containing plasmid. Encouragingly, Venken *et al.* developed the P[acman] system for the introduction of large DNA fragments into the fly genome using phiC31 and achieved integration of genomic fragments on the order of 100 kb with remarkable efficiencies (Venken *et al.* 2006). We took advantage of this technical innovation and set out to determine whether a preexisting *att* site could render a surrounding genomic region of similar size amenable to targeted modification. Our study reveals that modifying a genomic region 70 kb away from the attachment site can be quite efficient. In addition, both integration and reduction reactions for our large genomic fragment occurred at a frequency comparable to those previously achieved. Furthermore, reduction events could be recovered from spontaneous events that occur through meiotic recombination. We took the opportunity to introduce a new *att* site 70 kb downstream from the original one, further expanding the mutable region by at least another 70 kb. We propose to combine our targeting scheme with transposon-delivered *att* sites genome-wide to render all *Drosophila* genes amenable to targeted mutagenesis.

## Materials and Methods

Primer sequences are listed in Supporting Information, Table S1.

### *Construction of the pWalkman vector*

The unique *Nhe*I site in pP[acman] was used to introduce an *FRT* next to the 3′ inverted repeat of the *P* element as a product of annealing two oligos (NheFRT48-plus and NheFRT48-minus) with overhangs compatible to *Nhe*I. The unique *Sph*I site was used to clone an *FRT* next to the 5′ inverted repeat of the *P* element. The *FRT* oligos used were SphFRT48-plus and SphFRT48-minus. A clone was selected in which the two FRTs are in a directed orientation. The unique PmeI site in pP[acman] was used to clone an I-*Sce*I cut site with the oligos ScBaNhSpMlBsSb+ and ScBaNhSpMlBsSb−. This position corresponds to IS1 in Figure 1. The I-*Sce*I oligos also include restriction sites for *Bam*HI, *Nhe*I, *Sph*I, *Mlu*I, *Bsi*WI, and *Sbf*I enzymes immediately downstream of the I-*Sce*I cut site but upstream of the existing multiple cloning sites in pP[acman].

### *Construction of pWalkman{nbs-llp}*

A BAC clone (RP98-7E7) spanning the *nbs-llp* region was obtained from BacPac Resources (http://bacpac.chori.org). The gap repair method based on bacterial recombineering (Venken *et al.* 2006) was used to subclone the 82-kb *nbs-llp* region into the *Asc*I and *Eco*RI sites in pWalkman. A detailed description of cloning by recombineering, including the insertion of various DNA elements, can be found in Supporting Information, File S1.

### *Fly genetics*

The pWalkman constructs were injected into embryos with a *vasa*-driven phiC31 transgene (Bischof *et al.* 2007) and an *attP* insertion at *nbs* (Gao *et al.* 2008). Crossing schemes are presented in File S2.

## Results

### *Experimental design*

We previously used SIRT to create an allelic series for the *nbs* locus in *Drosophila* (Gao *et al.* 2008). To determine if the

same *attP* site could be used to modify a remote region, we set out to target a region ~70 kb from *nbs*.

We generated the pWalkman vector, which is based on the P[acman] vector system that was developed to facilitate cloning and large-scale production of plasmids containing large genomic inserts (Venken *et al.* 2006). pWalkman includes additional features to facilitate SIRT manipulation (Figure 1). First, a cut site for the rare cutting I-*Sce*I enzyme was added to allow for double-strand break (DSB)-induced reduction. I-*Sce*I is more advantageous as a choice of DSB-inducing enzyme than the I-*Cre*I used in previous reduction reactions because overproduction of I-*Cre*I reduces viability and fertility in flies (Rong *et al.* 2002). Second, two *FRT* sites were placed in a directed orientation to enable FLP-mediated excision of the plasmid backbone after plasmid integration. Finally, additional restriction sites were added to ease cloning of inserts.

While this targeting system could be used to mutate a specific gene, we chose instead to insert another attachment site at a distant "target region." We reasoned that this would create a valuable resource for those interested in using SIRT to modify their genes of interest in the vicinity of the new attachment site. We chose the region containing *CG8177*, *CG14168*, and a cluster of four *Ilp* genes as the target region for the new *att* site (from here on referred to as the *Ilp* locus). Since the integrating plasmid has an *attB* site at the *nbs* locus (*attB@nbs*), we decided to target an *attB* instead of an *attP* to the *Ilp* locus (*attB@Ilp*) that is 68 kb away from *attB@nbs*. Since the phiC31 integrase does not act on identical attachment sites, our design would eliminate any complications due to intramolecular recombination between sites on the same plasmid.

To generate the construct, the 82-kb genomic fragment from the *nbs-Ilp* region was subcloned into pWalkman, and *attB* sites were added to *nbs* and *Ilp* loci (Figure 1). All three cloning steps were accomplished by using bacterial recombineering (Copeland *et al.* 2001). In the final construct, which we named pWalkman{nbs-Ilp}, the 8-kb fragment to the left of *attB@nbs* and the 6.5-kb one to the right of *attB@Ilp* were included to extend the homology necessary for reduction of the target duplication by homologous recombination (Figures 1 and 2). We have constructed two versions of pWalkman {nbs-Ilp} in which the only difference is the placement of the I-*Sce*I cut site (IS). In pWalkman{nbs-Ilp}IS1, the I-*Sce*I cut site is at position IS1, while in pWalkman{nbs-Ilp}IS2, it is at position IS2 (Figure 1).

### An 80-kb tandem duplication

Embryo injections of the pWalkman{nbs-Ilp}IS1 construct yielded 60 fertile adults, and 3 of these produced red-eyed offspring, which indicates an integration frequency of 5% (3/60, Table 1). All red-eyed progeny (15 in total) were used to establish homozygous lines that were subjected to genetic and molecular characterization. Integration of the plasmid at *nbs* would place the *white* marker gene on chromosome 3, a result observed for all 15 lines. It would also generate a duplication of the 80-kb *nbs-Ilp* region with the left copy having an *attL* at *nbs* and the right copy having an *attR* at *nbs* (Figure 1). Since all four *att* elements (*attB*, *attP*, *attR*, *attL*) differ in size, we used PCR reactions with the same pair of flanking primers to identify each site. We present a sample of the results in Figure 1B. In addition to a wild-type (*wt*) line (lane 1), we used two additional control lines for the *nbs* PCR, including the starting line carrying *attP@nbs* (lane 4) and an integration line from our previous study (Gao *et al.* 2008) as a reference for the size of *attL* and *attR* sites (lane 2). While the starting line produced a PCR product of ~650 bp for *attP*, an integration line from this study yielded a doublet consisting of an ~600-bp product for *attL* and an ~750-bp product for *attR* (lane 5), a result identical to that obtained with a previous integration line (lane 2). At the *Ilp* locus, the *wt* line produced an ~800 bp product (lane 6). An integration line generated a doublet with an additional ~1050-bp product for *attB* (lane 7). These results were confirmed for 3 of the 15 lines that originated from two independent parents.

The rest of the lines did not pass this simple PCR test. Results from some of the PCR tests are shown in Figure S1. We propose that these lines resulted from rearrangement of the *nbs-Ilp* region. Such rearrangements can be brought about by multiple exchanges between *attB* and *attP* at the two loci on different homologous chromosomes or on sister chromatids. For example, once the plasmid was integrated at *nbs*, *attB@Ilp* could engage in a second round of phiC-31-mediated exchange with *attP@nbs* on the homologous chromosome since the plasmid-injected stock is homozygous for that *attP* insertion. Instead of further characterizing these events, we chose to focus our study on the integration lines that passed the PCR test.

### Target reduction induced by an I-SceI-generated DSB

To reduce the duplication to a single copy at the *nbs-Ilp* region, we followed a reduction procedure (File S2). We initiated reduction by inducing an I-*Sce*I cut in the vector sequences. If the repair of the resulting DSB proceeds through homologous recombination (HR) between the two *nbs-Ilp* copies, the repair product would be a single-copy locus (Figure 2). We previously observed that the plasmid backbone included in the phiC31-mediated integration decreased efficiency of reduction (Gao *et al.* 2008). For this reason, we performed a FLP-mediated excision of the vector backbone that is flanked by *FRT* sites (Figure 1) without deleting any sequence from the *white* marker, prior to proceeding with the reduction step.

Potential germline reduction events were recovered as white-eyed progeny. These progeny occurred in ~10% of germlines that carried both the duplication and a source of I-*Sce*I (Table 1). As I-*Sce*I-induced white loss happens in the mitotic component of the germline (Rong and Golic 2000; Rong *et al.* 2002), we established homozygous lines for only one *white* progeny from each white-producing germline to ensure that only independent events were being evaluated.

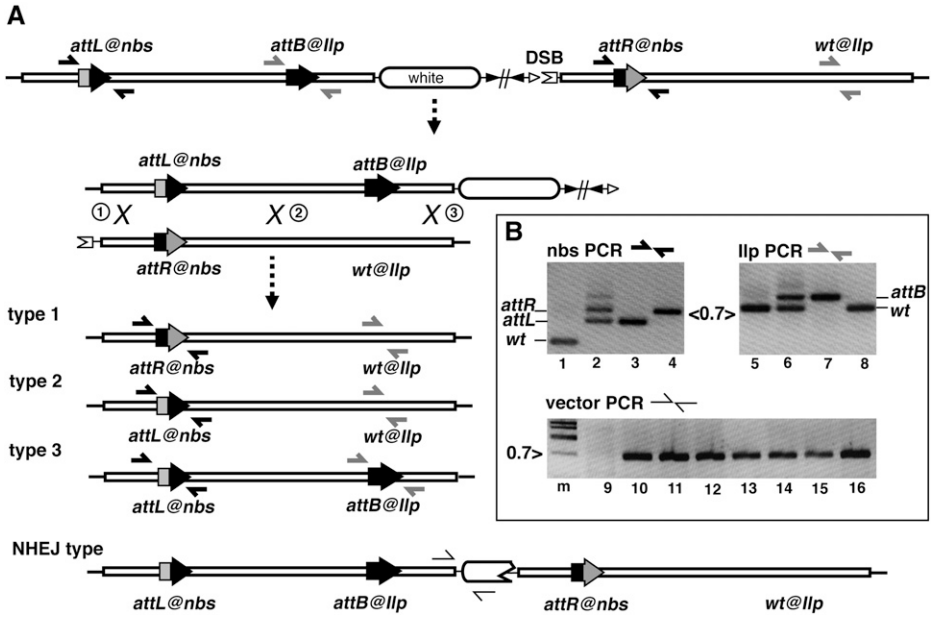


**Figure 2** I-*Sce*I-induced reduction. (A) Reduction schematic. At the top is the 80-kb duplication resulting from integration of pWalkman{nbs-Ilp}IS1. The I-*Sce*I endonuclease creates a DSB at IS1. The two *nbs-Ilp* regions align with three possible positions of recombination ("X"). The repair of the DSB gives rise to four types of events diagrammed below, with the first three being the product of recombination between the duplicated copies. The numbers in circles for the potential recombination sites correspond to the resulting types of reduction products. The positions of PCR primer sets are indicated (half arrows). In the NHEJ-type product, the *white* gene is disrupted ("broken" oval). The primer positions for "vector PCR" in B are indicated as half arrows. (B) Representative results for diagnostic PCR tests. The PCR templates for the top panels are the following: *wt* for lanes 1 and 5; a duplicated line for lanes 2 and 6; a type 3 reduction for lanes 3 and 7; a type 1 reduction for lane 4; and a type 2 event for lane 8. The 0.7-kb marker is indicated between the gel pictures. The PCR templates for the bottom panel are a reduction line for lane 9 and different NHEJ-type lines for lanes 10–16. Lane "m" represents markers with size indicated to the left in kilobases.

We verified the reduction outcomes for these lines using the same PCR strategy employed to verify the duplications (Figure 1). We expected that the single reduced copy would fall into three possible reduction types (Figure 2). If HR occurs within the 8-kb region to the left of *nbs*, the reduction would carry *attR@nbs* and be *wt* at the *Ilp* locus (reduction type 1). If HR occurs within the 68-kb region between *nbs* and *Ilp*, reduction would carry *attL@nbs* and be *wt* at *Ilp* (type 2). Only if HR occurs within the most distal 6.5 kb of the *nbs-Ilp* homology would it carry the desired *attB@Ilp* alongside *attL@nbs* (type 3). Representative products for these PCRs are shown in Figure 2B.

Table 1 summarizes the reduction results obtained from using the pWalkman{nbs-Ilp}IS1 construct. Six of 21 white-loss lines were precise reduction events based on PCR tests. Five of the 6 resulted from a type 1 reduction. The one exception resulted from a type 2 reduction. While we did not obtain any type 3 reduction events in this round, these desirable events were ultimately recovered in experiments described in the next section.

Unexpectedly, we observed a fourth but predominant type from our white-loss lines. For 15 of the 21 lines, the PCR results looked identical to those from the original duplication lines: a doublet in PCR tests for both the *nbs* and the *Ilp* loci. We hypothesized that these lines resulted from imprecise nonhomologous end joining (NHEJ) repair of the induced DSB where the *white* marker had suffered sequence loss before the break was ligated. This hypothesis was confirmed in 14 lines, in which a positive PCR result for the presence of vector sequences was evident (bottom panel in Figure 2B).

We have thus demonstrated two important aspects of this system that suggest that it will be easily applicable for gene targeting. First, we have found that reduction of an 80-kb duplication by DSB-induced HR can be efficient, with 10% of the males tested in our experiment resulting in white-loss events, of which 29% were reduction events. Second, we showed that the types of reduction events can be distinguished by a simple PCR test.

To provide further evidence supporting the accuracy of our PCR-based tests, we genotyped several lines from the reduction screen with regard to two single-nucleotide polymorphisms (SNPs) between the starting *nbs-Ilp* region on the chromosome and the same region, but originating from the BAC clone. We assayed a C/T SNP at position ~35 kb (p35) and a single T insertion/deletion SNP at position ~44 kb (p44) (see Figure 3 for approximate positions). As shown in Figure S2, both SNPs are heterozygous in nonreduced lines (NHEJ type), consistent with their carrying the duplication, while reduced lines are homozygous at both positions.

### *Effect of I-SceI cut-site placement on the recovery of reduction types*

Our inability to recover type 3 reduction events that retain *attB@Ilp* prompted us to consider whether the IS1 position for the I-*Sce*I cut site in pWalkman{nbs-Ilp}IS1 favors the recovery of type 1 reduction, in which the *Ilp* locus remains *wt*. To test this hypothesis, we generated the pWalkman {nbs-Ilp}IS2 construct that carries the I-*Sce*I cut site at position IS2, on the other side of *white* and closer to *attB@Ilp* than IS1. This new construct was then taken through the same series of experiments as pWalkman{nbs-Ilp}IS1 to recover *attB@Ilp* in the reduction events.

The integration frequency for pWalkman{nbs-Ilp}IS2 was 6% (14 independent events of 220 fertile crosses). As before, *white* mapped to the third chromosome in all 14 lines. Of the 10 lines that we tested by PCR, 3 showed PCR results

**Table 1 Frequency of reduction events**

| Construct[a] | Source of DSB[b] | White-loss frequency[c] | Reduction frequency[d] | Reduction type[e] | | |
|---|---|---|---|---|---|---|
| | | | | 1 | 2 | 3 |
| pWalkman{nbs-Ilp} | | | | | | |
| IS1 | I-*Sce*I | 10% (24/230) | 29% (6/21) | 5 | 1 | 0 |
| | P transposase | 13% (19/150) | 37% (7/19) | 6 | 1 | 0 |
| | Spontaneous[f] | | | | | |
| | Female | 0.1% (39/35,000) | 37/37 | 1 | 35 | 1 |
| | Female[g] | 0.1% (22/15,000) | 8/8 | 1 | 7 | 0 |
| | Male | 0.0% (0/8000) | 0 | | | |
| IS2 | I-*Sce*I | 13% (45/350) | 39% (13/33) | 6 | 1 | 6 |
| | Spontaneous[f] female | 0.1% (11/13,000) | 11/11 | 0 | 11 | 0 |

[a] Constructs used for site-specific integration.
[b] The source of DSB that led to the reported reductions.
[c] For induced events, the frequency was calculated by dividing the number of male parents yielding white-eyed progeny over the total number of males tested. The actual counts are included in parentheses. For spontaneous events, the frequency was calculated by dividing the number of white-eyed offspring over the total number of progeny. The counts are included in parentheses.
[d] Calculated by dividing the number of confirmed reductions over all white-loss events tested by molecular means.
[e] For the molecular structure of different types of reduction events, see Figure 2.
[f] Spontaneous events are categorized according to the gender of the duplication-carrying parents.
[g] Flanking recessive markers were used to demonstrate homolog exchanges (see text).

consistent with an un-rearranged duplication, and one of these lines was taken through the reduction procedure.

Table 1 shows the frequencies for reduction with the new construct. Recovery of white-loss events occurred at a similar frequency to that for the previous construct (13%, 45/350 germlines). As was observed previously, more than half (20/33) of the analyzed white-loss lines remained in a state of duplication (NHEJ type, Figure 2). Remarkably, this time the reaction was not biased against type 3 reduction, resulting in recovery of six lines carrying *attB@Ilp* out of 13 confirmed reduction events. Therefore, by putting the I-*Sce*I cut site on the side of the vector that is closer to the desired modification (*attB@Ilp*) with respect to *white*, we were able to improve its recovery in the final reduced locus from 0 to 46% (6/13).

We also wanted to determine whether an inhibition of NHEJ DSB repair would result in an increase in reduction frequency. For that purpose, we repeated the reduction procedure in a background mutant for DNA ligase 4 (*lig4*, File S2). Of 330 *lig4* mutant males tested, 49 gave white-eyed progeny (15%). Of 10 white-loss events tested by PCR, 2 were reduction events (20%), with both of them carrying the desired *attB@Ilp* modification. Therefore, the reduction frequencies recovered from the *lig4* mutant background are very similar to those obtained in *wt* males, suggesting that Ligase 4 is not essential for generating the NHEJ-type events in our system.

### *Reductions induced by P-element transposase*

As another way to initiate reduction, we explored the use of the *P*-element transposase to generate the DSBs. This strategy is possible because pWalkman sequences contain two *P*-element ends. Although these *P*-element ends are in an "inside-out" orientation when compared to their natural orientation, they can nevertheless be acted on by the P transposase to generate a DSB (Liang and Sved 2009). To test the efficacy of this approach, we introduced a source of P transposase into the duplicated lines and screened for potential reduction events as before. We observed a white-loss frequency of 13% and a bias toward type 1 reduction (Table 1), similarly to what we obtained using I-*Sce*I.

### *Recovering reduction by spontaneous recombination*

During the course of this study, we observed white-eyed progeny from flies carrying the 80-kb duplication without exposure to I-*Sce*I or the P transposase. We suspected that these events could result from spontaneous recombination between the copies in the *nbs-Ilp* region. We envisioned three possible modes of crossing over that could lead to the loss of *white*, including crossovers (1) between the two *nbs-Ilp* copies on the same chromatid, (2) between copies on sister chromatids but out of register, and (3) between copies on homologous chromosomes also out of register (unequal crossing over). To recover more of these spontaneous events for molecular analyses, we crossed female flies homozygous for the duplication to *white* males and looked for white-eyed individuals among the heterozygous progeny. Using the pWalkman{nbs-Ilp}IS1 construct, we recovered 39 *white* individuals from 35,000 offspring (~0.1%, Table 1). We tested 37 of these by the same PCR scheme as shown in Figure 1, and all were confirmed to be reduction events. One of them contained *attB@Ilp*. We also observed a strong bias toward one reduction type, specifically type 2 (35/37), which resulted from recombination within the 68-kb region between *nbs* and *Ilp*. We confirmed that spontaneous reductions occurred at the same rate of 0.1% in the germlines of females carrying the duplication made from the pWalkman {nbs-Ilp}IS2 construct. All 11 recovered events resulted from a type 2 reduction. In our previous experience with SIRT at the *nbs* locus, we did not observe any spontaneous white-loss events. However, our prior experimental setup included a smaller 5.5-kb duplication of the region (Gao

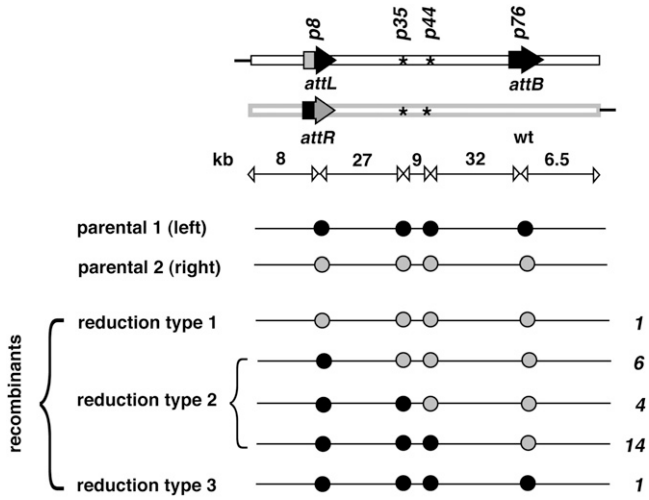


**Figure 3** Spontaneous products are crossovers between the two duplicated copies. The two parental copies of the *nbs-Ilp* region are shown on the top with the four pieces of sequence heterology labeled according to their approximate distance from the left end of the *nbs-Ilp* region. The physical distance between heterologous sites is shown in kilobases below the diagram for the parental copies. (Bottom) Another representation of the *nbs-Ilp* parental copies and their five crossover products with each heterology depicted as a solid circle. The three types of reduction product have been defined in Figure 2. The number to the right of each product represents the number of lines identified for each outcome.

*et al.* 2008). Our results here suggest that the presence of a larger duplication can induce another means to recover reduction products via spontaneous recombination.

### *Spontaneous events are results of meiotic recombination*

We hypothesized that the spontaneous recombination events observed in our screen resulted from unequal crossing over between homologous chromosomes in meiosis. We made two observations consistent with this hypothesis. First, most of the events (35/37) were of type 2, which arise from crossovers within the largest portion of homology between the two duplicated copies (68 of 82 kb). Second, we did not observe any presumed NHEJ type events (Table 1), which is consistent with the fact that NHEJ is not a major pathway for the repair of meiotic DSBs (Joyce *et al.* 2012).

Nonetheless, the nature of the spontaneous events could be accounted for by both mitotic and meiotic events. We set out to further distinguish between these two possibilities. First, a similar screen did not yield any white-eyed events in 8000 progeny from males homozygous for the duplication (Table 1). This is consistent with the fact that meiotic recombination is limited to *Drosophila* females. Second, we found that spontaneous reduction events are always accompanied by the exchange of flanking markers on homologous chromosomes, a hallmark of meiotic recombination. To track the exchange of flanking markers, we generated females homozygous for the *nbs-Ilp* duplication and heterozygous for markers on the centromere-distal side of the duplication and on the centromere proximal side. In these females, one duplication carries the *hairy*[1] (*h*[1]) distal mutation but is wild type at the proximal locus of *approximated* (*app*$^+$), while the other duplication carries $h^+$ and *app*[1]. Females of this genotype were used to set up the screen for spontaneous reductions. All resulting reduction events were crossed to flies homozygous for both *h*[1] and *app*[1] to assay the mutation status on the reduced chromosome. All 23 events carried either both or neither of the flanking recessive mutations, indicating that the flanking regions of the homologs were exchanged. Taken collectively, these results serve as strong evidence that the spontaneous events result from unequal crossing over in meiosis.

### *Mapping points of meiotic crossing over*

The large number of recombinant lines that we recovered within the 82-kb interval presented us with an opportunity to investigate whether the crossing-over points are clustered within a relatively small interval. We arbitrarily divided the 82-kb region into five subregions using four pieces of heterology between the duplicate copies (Figure 3). At position 8 kb (p8) from the left end of the *nbs-Ilp* genomic fragment is the *attR/attL* heterology at *nbs*. At positions 35.1 kb (p35) and 43.7 kb (p44) there is a pair of previously described SNPs (Figure S2). At position 75.6 kb (p76) is the *attB* heterology at *Ilp*. Reduction homozygotes were genotyped with regard to the four heterologous locations. The results are shown in Figure 3. As expected for the type 1 event, all four sites of heterology correspond to the right copy in the duplication (*i.e.*, parental 2), while for the type 3 event they correspond to the left copy (*i.e.*, parental 1). For type 2 events, we recovered crossovers within all three regions of the 68 kb subdivided by the sites of heterology. Although the crossing-over frequency within this region is not strictly proportional to the extent of homology, we did not observe any region with a crossing-over rate that is greatly disproportional to the extent of homology.

## Discussion

We have previously demonstrated that the SIRT method greatly facilitates targeted manipulation of genes situated close to a previously targeted phiC31 integrase attachment site (Gao *et al.* 2008, 2011). We hypothesized that this principle can be applied to genes farther away from that attachment site with the use of a larger DNA fragment. Here we provided a proof-of-principle study by modifying a region situated almost 70 kb from an existing attachment site. Our results lead us to propose this procedure as a strategy for accessing new genes for repeated mutagenesis.

### *Long-distance targeted modification*

Although phiC31-mediated insertion of large DNA fragments at ectopic positions occurs at a frequency of 2–4% for constructs >50 kb (Venken *et al.* 2006), we were uncertain of whether such a frequency could be achieved when inserting a large fragment at its endogenous location because of potential instability of the resulting large duplication. This concern

was resolved when we recovered integrations at a frequency of 5% or greater and were able to maintain the stocks indefinitely.

Interestingly, we observed infrequent spontaneous reduction events in female germlines homozygous for the duplication. Unequal meiotic crossing over between tandem duplications has been previously observed in many cases (*e.g.*, Green 1962). We provided evidence that spontaneous reduction in our system happens through a similar mechanism. The genetic crosses for the recovery of spontaneous events are quite simple, making it an attractive alternative to the I-*Sce*I-induced mitotic recombination method. In addition, the elimination of the NHEJ-type events simplifies PCR testing. However, this might not be a viable option when dealing with genomic regions with an intrinsically low meiotic recombination frequency.

Our previous experiences in reducing tandem duplications with a site-specific DSB all involved small duplications of a few kilobases in size (Rong *et al.* 2002; Gao *et al.* 2008, 2011). Here we faced the question of whether the efficiency of reducing a large duplication by a site-specific DSB would not drop to a prohibitive level. When comparing with our previous results, we observed a substantial drop in white-loss events (from 77–100% to 10–13%) and a substantial increase in NHEJ repair products (from essentially 0% to 60–70%). Nevertheless, our results remain rather encouraging. For the 10–13% of germlines that did experience white loss, about one-third of the white-loss events (29–39%) are reduction events. This translates to about one reduction event for every 30 male germlines tested. More importantly, the goal of our study was to recover not only reduction events of the duplication, but also the specific event with our desired modification, *i.e.*, *attB@Ilp*. Around 46% of the reduction events from experiments using the pWalkman{nbs-Ilp}IS2 construct retain *attB@Ilp*. Therefore, a desired reduction event could be recovered for every 65 (30/0.46) males tested.

### *Recombination mechanisms for the reduction of large duplications*

When comparing the efficiency of *attB@Ilp* retention in the reduction product, we obtained startlingly different results with two different vector configurations depending on which side of the *white* gene the future DSB site was placed (Figure 1 and Table 1). For construct pWalkman{nbs-Ilp}IS2, in which the I-*Sce*I cut site is physically closer to *attB@Ilp* with respect to *white*, nearly half of the reduction events retained *attB@Ilp*. Remarkably, none of the six events retained *attB@Ilp* when recovered with pWalkman{nbs-Ilp}IS1, in which the I-*Sce*I cut site is farther away from *attB@Ilp*. This result is also observed when using P transposase as a means of generating the DSB, most likely due to similar positioning of the DSB to the one generated by I-*Sce*I at position IS1 (see Figures 1 and 2 for the position of *P*-element ends in the duplication). This preference in regard to the placement of the DSB is opposite to that previously observed when much smaller duplications were tested (Rong *et al.* 2002; Gao *et al.* 2008). The previous results are consistent with reduction occurring via the DSB repair mechanism of single strand annealing (SSA), which is the predominant mechanism for repairing a DSB flanked by direct repeats of a few kilobases in size (Rong and Golic 2003; Wei and Rong 2007). In SSA, both ends of the DSB experience single-strand resection at the 5′ to 3′ direction. Resection has to be sufficiently extensive to expose complementary single-stranded regions between the two repeats. Annealing of the two regions followed by trimming of the protruding single-stranded tails complete the repair process, thus reducing the two copies to one. Thus, SSA repair would result in the preferential loss of sequence heterology closer to the DSB (Figure 4A).

For reducing large duplications, SSA is unlikely to be the major mechanism, simply due to the extent of resection required. In our case, resection of both ends would encompass at least 82 kb of *nbs-Ilp* plus 5 kb of *white* sequences. Instead, we propose that a significant portion of the reduction events that we recovered were the result of a "one-ended invasion crossover" mechanism, which has been previously invoked to account for repair products during spontaneous recombination between two direct repeats in yeast (Prado and Aguilera 1995). We envision that resection of the DSB end proximal to one of the repeats would expose single-strand homology leading to that end invading the homologous region in the other repeated copy (Figure 4B). This one-ended invasion ultimately leads to the resolution of a single Holliday junction and the appearance of the reduction product (for a detailed description of the model, see Figure 4 in Prado and Aguilera 1995). This model predicts that sequence heterology that is proximal to the DSB (*e.g.*, *attB@Ilp*) would be part of the invading end and be more likely to be retained in the reduction product. On the other hand, heterology separated from the DSB end by vector sequences would be less likely to be retained. This is consistent with our inability to recover events that retained *attB@Ilp* when construct pWalkman{nbs-Ilp} IS1 was used to create the duplication and with the preferred recovery of *attR@nbs* (type 1 reduction in Figure 2). On the other hand, *attB@Ilp* was efficiently recovered when pWalkman{nbs-Ilp}IS2 was used. We did recover cases in which *attB@Ilp* was not retained even with this favorable configuration. Further investigation is needed to shed light on the repair mechanisms responsible for these reduction products.

Based on these results, we suggest that, for reducing a large duplication, the genomic insert within the pWalkman vector should be oriented in such a way as to place the I-*Sce*I site closer to the end of the insert that carries the modification, similar to the IS2 position in Figure 1. In addition, because the FLP-catalyzed vector excision would not be necessary, using P transposase might be a simpler way to induce reduction.

### *Toward genome-wide targeted manipulations in Drosophila*

The goal of knocking out every gene in *Drosophila* has been a long-lasting crusade for the fly community (Bellen *et al.* 2011). A significant portion of the 15,000 annotated genes

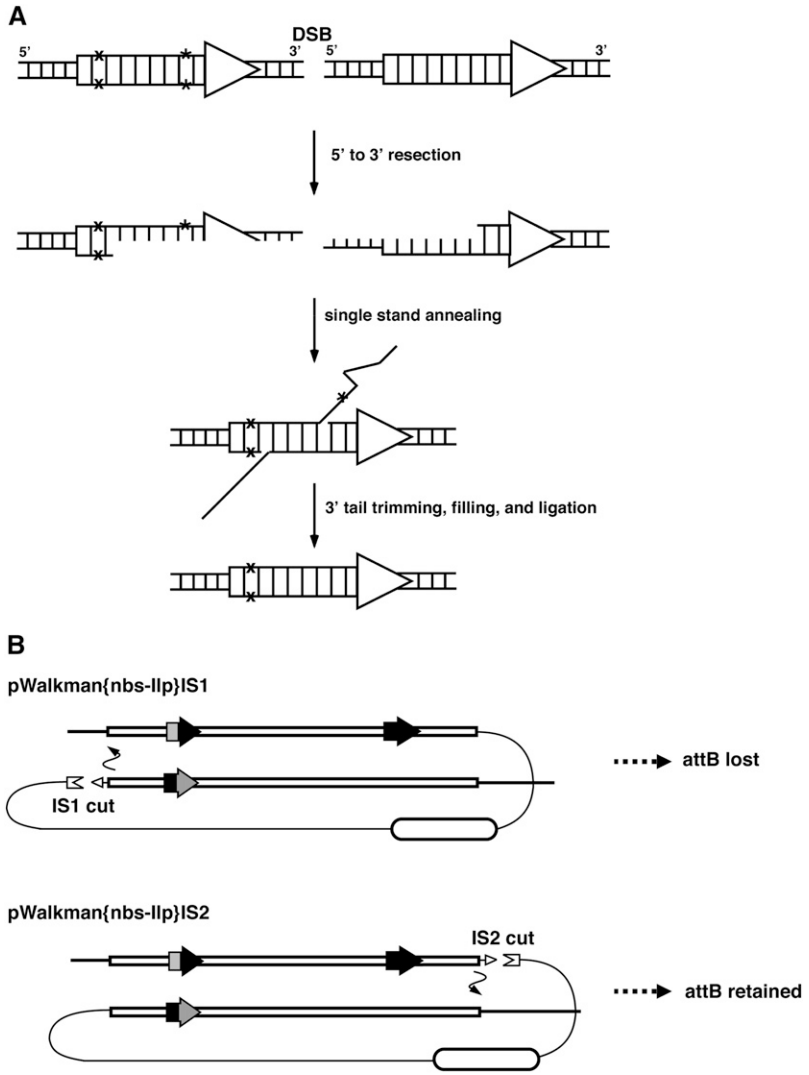


**Figure 4** The effects of different repair mechanisms on reduction outcomes. (A) SSA repair as the mechanism for reduction. (Top) A DSB has been induced between two direct repeats (block arrows) with each horizontal line representing a DNA strand and vertical lines representing base pairing. The two heterologies between the repeats are denoted by an "X" and by an asterisk. The heterology indicated by the asterisk is more likely to become single stranded and thus excluded from the final reduction product due to its being closer to the DSB. (B) The "one-ended invasion crossover" model as the mechanism for reduction. The 80-kb duplication is shown for both pWalkman {nbs-llp} constructs. In the top diagram, IS1 is cut and the right end of the DSB in the bottom copy invades the homologous sequences of the top copy, leading to loss of the *attB* heterology. In the bottom diagram, IS2 is cut and the left end of the DSB in the top copy invades homologous sequences of the bottom copy, leading to retention of the *attB*. Note that in either case the invaded copy can be located on the sister chromatid instead.

still lack defined mutations after a century of random mutagenesis in *Drosophila*. The invention of a reliable gene targeting method by Rong and Golic in 2000 opened the possibility for disrupting every fly gene by homologous recombination. However, gene targeting in complex organisms is inherently labor intensive and time-consuming, making its genome-wide application a daunting task. In addition, the return from a genome-wide knock-out collection is limited, as it provides only a single allele for each gene. Yet systematic mutational studies become increasingly important for our complete comprehension of gene function. Thus, even with the availability of a genome-wide knock-out collection, subsequent modifications of a particular gene have to be introduced as transgenes at ectopic loci and might be under the influence of chromosome position effects that are not well understood.

We suggest, as an alternative, the creation of a collection of fly lines carrying *att* sites distributed throughout the whole genome, which would enable unlimited rounds of targeted manipulations for essentially all genes. If we consider that any *att* site creates a point of access to ~140 kb of the surrounding DNA (70 kb in each direction), then the 160 Mb of the fly genome could be covered with 1200 different *att* stocks. We propose that transposable elements can be utilized to distribute the *att* sites throughout the genome. Progress in this regard has already been made with the availability of independent collections, such as the MiMIC lines (Venken *et al.* 2011). Our method will be additionally advantageous in two ways. First, it can be used to modify a region 70 kb or less from an existing *att* site. Second, it can be used to fill large gaps void of any *att* site (hence the name "Walkman" for our vector). The estimated number of 1200 new stocks represents a small burden if we consider that, in 2010, the Bloomington Stock Center alone reported holding 38,000 different stocks. The potential utility of these ~1200 stocks would be unprecedented. Once any locus is equipped with a proximal *att* site, the possibilities for further modification by SIRT are endless.

## Acknowledgments

We are grateful to Flavia Amariei for aiding us with screening for spontaneous reductions and to Jemima Barrowman for her assistance in editing the manuscript. Research in our laboratory

is supported by the Intramural Program of the National Cancer Institute.

## Literature Cited

Bellen, H. J., R. W. Levis, Y. He, J. W. Carlson, M. Evans-Holm *et al.*, 2011 The *Drosophila* gene disruption project: progress using transposons with distinctive site specificities. Genetics 188: 731–743.

Bischof, J., R. K. Maeda, M. Hediger, F. Karch, and K. Basler, 2007 An optimized transgenesis system for Drosophila using germ-line-specific phiC31 integrases. Proc. Natl. Acad. Sci. USA 104: 3312–3317.

Copeland, N. G., N. A. Jenkins, and D. L. Court, 2001 Recombineering: a powerful new tool for mouse functional genomics. Nat. Rev. Genet. 2: 769–779.

Gao, G., C. McMahon, J. Chen, and Y. S. Rong, 2008 A powerful method combining homologous recombination and site-specific recombination for targeted mutagenesis in Drosophila. Proc. Natl. Acad. Sci. USA 105: 13999–14004.

Gao, G., Y. Cheng, N. Wesolowska, and Y. S. Rong, 2011 Paternal imprint essential for the inheritance of telomere identity in Drosophila. Proc. Natl. Acad. Sci. USA 108: 4932–4937.

Gloor, G. B., N. A. Nassif, D. M. Johnson-Schlitz, C. R. Preston, and W. R. Engels, 1991 Targeted gene replacement in Drosophila via P element-induced gap repair. Science 253: 1110–1117.

Gong, W. J., and K. G. Golic, 2003 Ends-out, or replacement, gene targeting in Drosophila. Proc. Natl. Acad. Sci. USA 100: 2556–2561.

Green, M. M., 1962 The effects of tandem duplications on crossing over in Drosophila melanogaster. Genetica 33: 154–164.

Gronke, S., D. F. Clarke, S. Broughton, T. D. Andrews, and L. Partridge, 2010 Molecular evolution and functional characterization of Drosophila insulin-like peptides. PLoS Genet. 6: e1000857.

Groth, A. C., M. Fish, R. Nusse, and M. P. Calos, 2004 Construction of transgenic Drosophila by using the site-specific integrase from phage phiC31. Genetics 166: 1775–1782.

Huang, J., W. Zhou, W. Dong, and Y. Hong, 2009 Targeted engineering of the Drosophila genome. Fly (Austin) 3: 274–277.

Iampietro, C., M. Gummalla, A. Mutero, F. Karch, and R. K. Maeda, 2010 Initiator elements function to determine the activity state of BX-C enhancers. PLoS Genet. 6: e1001260.

Joyce, E. F., A. Paul, K. E. Chen, N. Tanneti, and K. S. McKim, 2012 Multiple barriers to nonhomologous DNA end joining during meiosis in *Drosophila*. Genetics 191: 739–746.

Liang, X., and J. A. Sved, 2009 Repair of P element ends following hybrid element excision leads to recombination in Drosophila melanogaster. Heredity (Edinb) 102: 127–132.

Prado, F., and A. Aguilera, 1995 Role of reciprocal exchange, one-ended invasion crossover and single-strand annealing on inverted and direct repeat recombination in yeast: different requirements for the RAD1, RAD10 and RAD52 genes. Genetics 139: 109–123.

Rong, Y. S., and K. G. Golic, 2000 Gene targeting by homologous recombination in Drosophila. Science 288: 2013–2018.

Rong, Y. S., and K. G. Golic, 2003 The homologous chromosome is an effective template for the repair of mitotic DNA double-strand breaks in Drosophila. Genetics 165: 1831–1842.

Rong, Y. S., S. W. Titen, H. B. Xie, M. M. Golic, M. Bastiani *et al.*, 2002 Targeted mutagenesis by homologous recombination in D. melanogaster. Genes Dev. 16: 1568–1581.

Spitzweck, B., M. Brankatschk, and B. J. Dickson, 2010 Distinct protein domains and expression patterns confer divergent axon guidance functions for Drosophila Robo receptors. Cell 140: 409–420.

Venken, K. J., Y. He, R. A. Hoskins, and H. J. Bellen, 2006 P[acman]: a BAC transgenic platform for targeted insertion of large DNA fragments in D. melanogaster. Science 314: 1747–1751.

Venken, K. J., K. L. Schulze, N. A. Haelterman, H. Pan, Y. He *et al.*, 2011 MiMIC: a highly versatile transposon insertion resource for engineering Drosophila melanogaster genes. Nat. Methods 8: 737–743.

Wei, D. S., and Y. S. Rong, 2007 A genetic screen for DNA double-strand break repair mutations in Drosophila. Genetics 177: 63–77.

Weng, R., Y. W. Chen, N. Bushati, A. Cliffe, and S. M. Cohen, 2009 Recombinase-mediated cassette exchange provides a versatile platform for gene targeting: knockout of miR-31b. Genetics 183: 399–402.

*Communicating editor: J. Sekelsky*

GENETICS

**Supporting Information**
http://www.genetics.org/content/early/2012/11/06/genetics.112.145631/suppl/DC1

# Long-Range Targeted Manipulation of the *Drosophila* Genome by Site-Specific Integration and Recombinational Resolution

**Natalia Wesolowska and Yikang S. Rong**


DOI: 10.1534/genetics.112.145631

**File S1**

**Supporting Text**

**Cloning of the 82kb insert by recombineering-mediated gap repair**

Primers bacL-f and bacL_NotI-r (with a 3' NotI site) were used to amplify a 500bp left arm of homology, and primers bacR_NotI-f (with a 5' NotI site) and bacR-r were used to amplify a 500bp right arm of homology. The two arms were ligated after NotI digestion, and AscI and EcoRI sites were added by a second round of PCR with bacL_AscI-f and bacR_EcoRI-r. The resulting 1000 bp product, flanked by AscI and EcoRI, was cloned into pWalkman and used for gap repair. To verify the integrity of the BAC fragment throughout the construction, 10 PCR primer pairs spaced evenly throughout the 80 kb were used (see Table S1C for their sequences). The final construct was also verified by restriction digest analyses with several enzymes: SalI, KpnI, NotI, BamHI and sequencing of cloning junctions.

**Insertion of DNA elements by recombineering**

The insertion of *attB@nbs* and *attB@Ilp* were accomplished with bacterial recombineering using the *galK* positive-negative selection system (WARMING *et al.* 2005) essentially as described on the website http://redrecombineering.ncifcrf.gov/. Briefly, we generated the *galK* insert by PCR, using primers with flanking homology to the *nbs* region – nbsGalk-f and nbsGalk-r. This fragment was inserted at *nbs* at the position identical to that of the *attP* in the nbs-attP line (GAO *et al.* 2008) in the construct pWalkman{nbs-Ilp}, and clones were selected on galactose plates. Subsequently, *galK* was replaced by an *attB* insert with *nbs* flanking homology. Primers nbs2776-f and nbs3169-r were used to amplify *attB@nbs* from an existing construct (GAO *et al.* 2008). After the second round of recombineering, cells that retained *galK* were selected against on deoxygalactose plates. A similar procedure was followed for *attB@Ilp,* which was placed within the intergenic region between CG8177 and CG14168. The following primers were used to insert GalK: bac810Galk-f and bac810Galk-r; and attB: bac810_attB-end with bac810_attB-head. The success of *attB* placement in each case was verified by sequencing.

For I-SceI cut site insertion at position IS2, the I-SceI cut site at IS1 (described previously) was first removed by *galK* selection and replaced with original sequences in pP[acman]. Subsequently, a cut site was inserted at the new position, again using *galK* selection. The primers used were: up7993Galk-f and dn7993Galk-r for inserting *galK* at IS1; acman7929-f and acman8029-r for restoring IS1 site to pP[acman] sequences; up8150Galk-f and dn8150Galk-r for inserting *galK* at IS2. To insert the cut site at IS2, oligos up8150IS2-f and dn8150IS2-r were annealed and converted to dsDNA by a single round of DNA synthesis. This DNA was then used as template in a PCR with primers up8150IS2plus-f and dn8150IS2plus-r to generate PCR product used to replace *galK* at IS2.

**File S2**
**Crossing schemes for induced reduction**

**I. Reduction by ISceI**

1. FLP-mediated excision of vector sequences

*w P[ry$^{+}$, 70Flp]; Sb/TM6* (F) **X** *w; Dp(3;3)nbs-Ilp,w$^{+}$* (M)

progeny heat shocked at 37**°**C for 1 hour

*w; Dp(3,3)nbs-Ilp$^{flipped}$,w$^{+}$/TM6*

2. Reduction by I-SceI cutting

2.1. *I-SceI* on chromosome 2

*w; Dp(3,3)nbs-Ilp$^{flipped}$,w$^{+}$ Sb/TM6B* (M) **X** *w; P[v$^{+}$, 70I-SceI] Sco/CyO* (F)

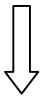

progeny heat shocked at 37**°**C for 1 hour

*w; P[v$^{+}$, 70I-SceI] Sco/+; Dp(3,3)nbs-Ilp$^{flipped}$,w$^{+}$ Sb/+* (M) **X** *w; TM3/TM6B* (F)

Scored *Sb* progeny for *w* and established lines

2.2. *I-SceI* on chromosome 3 (with *ligase 4* mutation)

*w; Dp(3,3)nbs-Ilp$^{flipped}$,w$^{+}$* (M) **X** *w lig4$^{11}$; P[v$^{+}$, 70I-SceI] Sb/TM6B* (F)

progeny heat shocked at 37**°**C for 1 hour

*w lig4$^{11}$; Dp(3,3)nbs-Ilp$^{flipped}$,w$^{+}$/P[v$^{+}$, 70I-SceI] Sb* (M) **X** *w; TM3/TM6B* (F)

Scored *Sb$^{+}$* progeny for *w*, and established lines

**II. Reduction by P transposase**

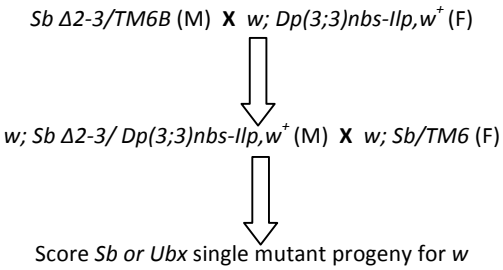


**Legend:**

M and F stand for male and female respectively. A heat shock treatment to the progeny was administered on day 3 after the cross had been set up. *Dp(3,3)nbs-Ilp,w*$^{+}$ indicates the 82kb duplication (*Dp*) of the *nbs-Ilp* region marked with *white*$^{+}$. *Dp(3,3)nbs-Ilp*$^{flipped}$*,w*$^{+}$ denotes the same duplication but with vector sequences excised by FLP recombinase. We did not verify the excision of the vector nor established an "excised" stock as FLP has been shown to function at virtually 100% efficiency under these conditions (GOLIC and LINDQUIST 1989, WEI and RONG 2007). p*P[ry*$^{+}$*, 70FLP]* is a *hsp70* promoter-driven *FLP* transgene on the X chromosome (GOLIC and LINDQUIST 1989). p*P[v*$^{+}$*, 70I-SceI]* is a *hsp70* promoter-driven *I-SceI* tansgene (RONG and GOLIC 2003). We used one insertion on chromosome 2 marked with *Sco* and one on chromosome 3 marked with *Sb*. The *lig4*$^{11}$ mutation was previously described (WEI and RONG 2007). A P transposase source is denoted as *Δ2-3*.

**References**

GAO, G., C. MCMAHON, J. CHEN and Y. S. RONG, 2008 A powerful method combining homologous recombination and site-specific recombination for targeted mutagenesis in Drosophila. Proc Natl Acad Sci U S A **105:** 13999-14004.

GOLIC, K. G., and S. LINDQUIST, 1989 The FLP recombinase of yeast catalyzes site-specific recombination in the Drosophila genome. Cell **59:** 499-509.

RONG, Y. S., and K. G. GOLIC, 2003 The homologous chromosome is an effective template for the repair of mitotic DNA double-strand breaks in Drosophila. Genetics **165:** 1831-1842.

WARMING, S., N. COSTANTINO, D. L. COURT, N. A. JENKINS and N. G. COPELAND, 2005 Simple and highly efficient BAC recombineering using galK selection. Nucleic Acids Res **33:** e36.

WEI, D. S., and Y. S. RONG, 2007 A genetic screen for DNA double-strand break repair mutations in Drosophila. Genetics **177:** 63-77.

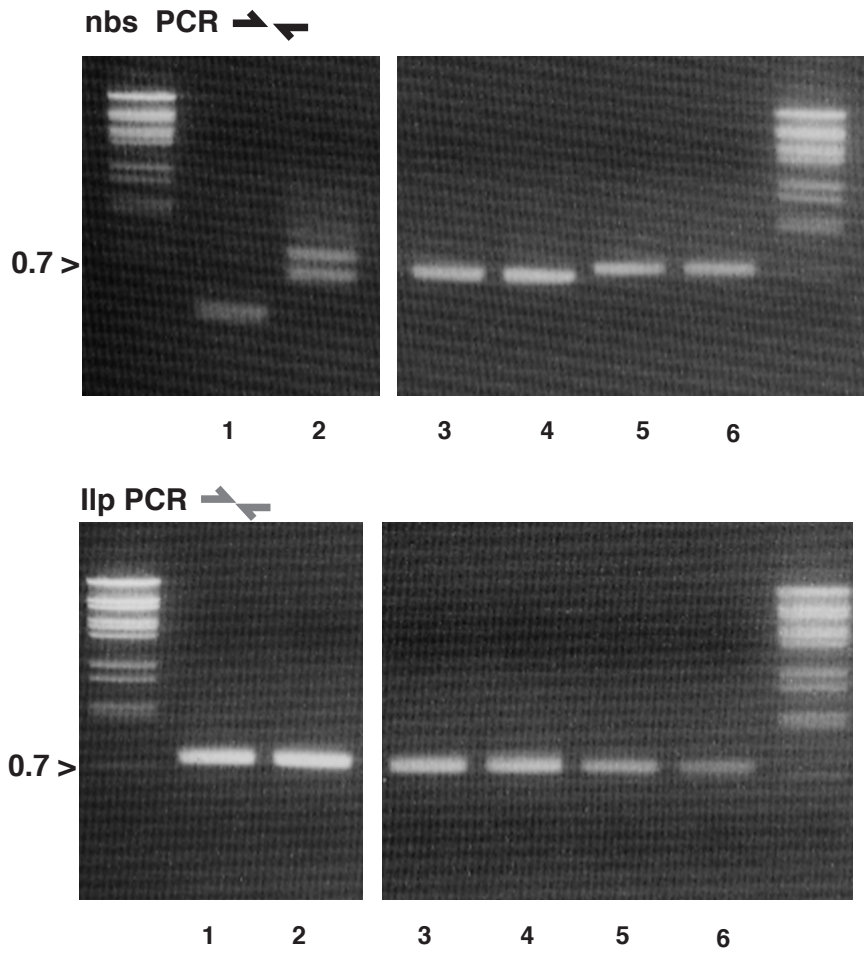


**Figure S1 Integration lines with possible rearrangement of the *nbs-llp* region.** Representative results for diagnostic PCR tests of integration lines showing abnormal patterns. Marker size is indicated to the left of the gel pictures in kb. At the top is the PCR test for the *nbs* region (for primer locations see Figure 1). At the bottom is the PCR test for the *llp* region. Lane 1: *wt*; lane 2: a duplication line from a previous integration at *attP@nbs*; lanes 3-6: additional integration lines from pWalkman{nbs-llp}IS1 integration. Note that the absence of the *attB@llp* band in the lanes 3-6 suggests that the *attB* might have participated in an additional round of phiC31-mediated recombination.

**SNP at p35**
PCR with primer pair bac416
sequenced with primer bac416r


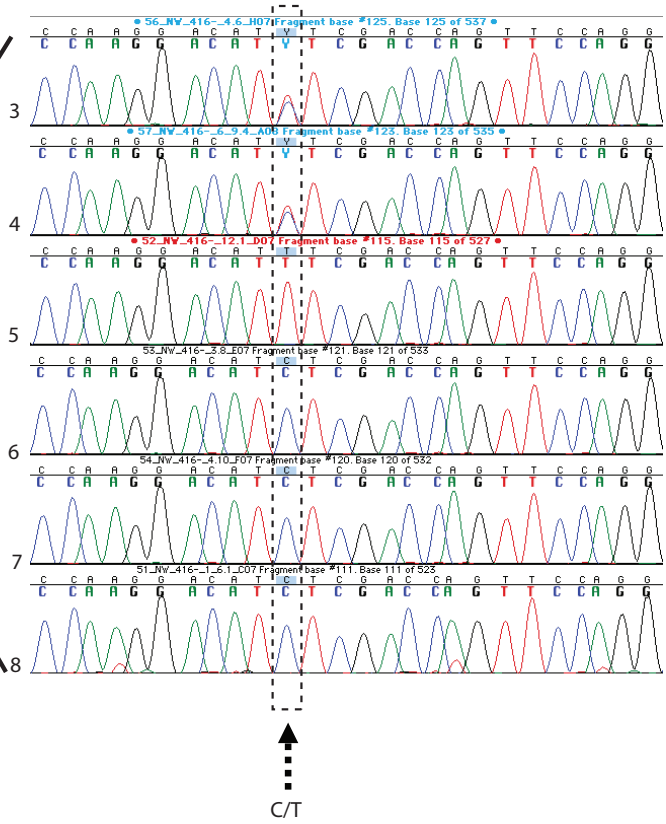


**indel at p44**
PCR with primer pair bac502
sequenced with primer bac502f

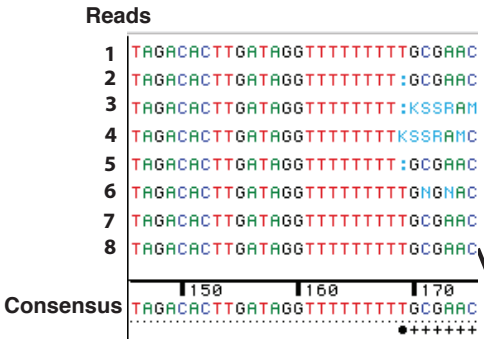


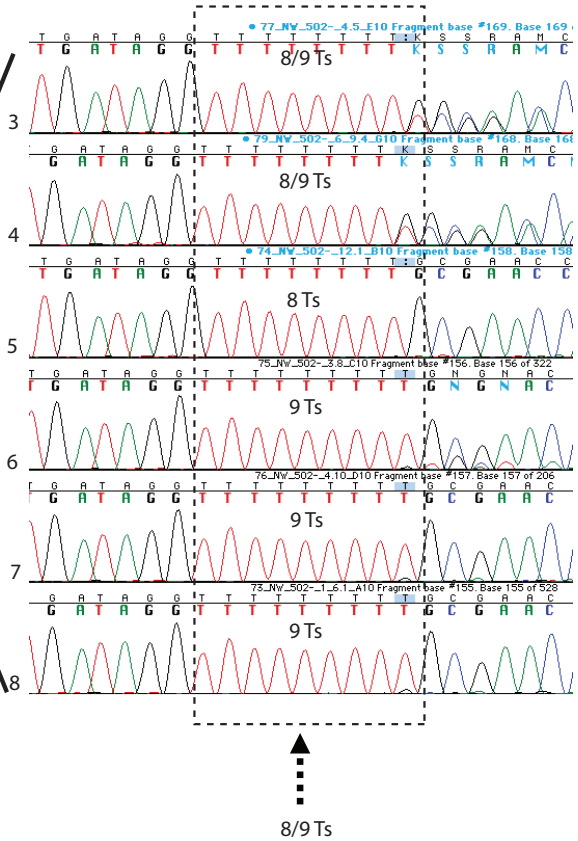

**Figure S2 Genotyping SNPs in reduction events.** Genotyping of the C/T SNP at position p35 is shown at the top. Sequences around the SNP region are shown for eight samples. Sample 1 was PCR amplified from pWalkman{nbs-Ilp} plasmid DNA showing a "C" at p35. Sample 2 was PCR amplified from genomic DNA of the starting line with *attP@nbs* showing a "T" at position p35. Samples 3 and 4 were amplified from genomic DNA of two NHEJ type lines (Figure 2). The sequencing data shown at the right displays a C/T double peak suggesting that both *nbs-Ilp* copies are present, which is consistent with NHEJ type events not being reduced. Samples 5-8 were derived from four lines that have been classified as "reduced" based on the PCR tests shown in Figures 1 and 2. Either a "C" or a "T" single peak was displayed in the sequencing data, consistent with the presence of a single *nbs-Ilp* copy. Genotyping of the T indel SNP at position p44 is shown at the bottom. The samples are the same as the ones used for genotyping p35. At this position, the *nbs-Ilp* region derived from the BAC clone (sample 1) has a string of nine "Ts", while the chromosomal copy has eight (sample 2). For samples 3 and 4 (NHEJ type), the deletion of a single "T" resulted in the appearance of a double peak for all bases downstream of the indel, due the presence of both *nbs-Ilp* copies. For reduced samples (samples 5-8), the indel is homozygous, again consistent with the presence of only one *nbs-Ilp* copy.

**Table S1 Primers used for plasmid construction, gap repair, verification PCRs and PCR assays**

| **A. Primers used for plasmid construction** | |
|---|---|
| **primer name** | **sequence** |
| ScBaNhSpMlBsSb+ | tagggataacagggtaatggatccgctagcatgcacgcgtacgcctgcagg |
| ScBaNhSpM1BsSb- | cctgcaggcgtacgcgtgcatgctagcggatccattaccctgttatcccta |
| NheFRT48-plus | ctaggaagttcctatactttctagagaataggaacttcggaataggaacttc |
| NheFRT48-minus | ctaggaagttcctattccgaagttcctattctctagaaagtataggaacttc |
| SphFRT48-plus | gaagttcctatactttctagagaataggaacttcggaataggaacttccatg |
| SphFRT48-minus | gaagttcctattccgaagttcctattctctagaaagtataggaacttccatg |
| **B. Primers used for gap repair** | |
| **primer name** | **sequence** |
| bacL-f | GCGGAGTTTCGATAAACAAAG |
| bacL_**NotI**-r | ctcaa**gcggccgc**CTACGATAACAAACACCTGCCC |
| bacL_**AscI**-f | gtcaa**ggcgcgcc**GCGGAGTTTCGATAAACAAAG |
| bacR-r | CTCGGCTATCTCGACTATCTCG |
| bacR_**NotI**-f | gacaa**gcggccgc**CTCGAGGTCGTTTGTGGTTTGTG |
| bacR_**EcoRI**-r | cagtt**gaattc**CTCGGCTATCTCGACTATCTCG |
| **C. Primers used for verification of nbs-llp region integrity during cloning** | |
| **primer name** | **sequence** |
| bac074-f | gtatcgggatgcatcgaagt |
| bac074-r | agagaaaatggccggagaat |
| bac064-f | gctccaatcgtcctcatcat |
| bac064-r | caggtgtgttgggggaatac |
| bac165-f | AGCCGGTTTGTTTTTGTGTC |
| bac165-r | CTCGACGGTATCGTGGCTAT |
| bac267-f | TCTACGTCATGGAGCACGAG |
| bac267-r | ATTCATGGTTCCAGCGTCTC |
| bac320-f | TCTTGAACTGCAGCACATCC |
| bac320-r | CAACAACATGGGGCACTAGA |
| bac416-f | CTCCCGACTCAACACCGTAT |
| bac416-r | CCAGCTATGCCAAGTTCACA |
| bac502-f | AGCAATACCAGGGGACAGTG |
| bac502-r | AACGAAACGTAACCGACAGG |
| bac600-f | TCGTCGATCTCTGGGTCTTT |
| bac600-r | AGGCGTGAATAATGCGATTC |
| bac729-f | ACGAGAAGCACGTCCAGTTT |
| bac729-r | TCTGTTCATTGGGGCTAAGG |
| bac835-f | AGGATGGAGGCTTGAGGATT |

| | |
|---|---|
| bac835-r | TTATCCCGGAATGCTTTGAG |

**D. Primers used for verification of gap repair junctions**

| **primer name** | **sequence** |
|---|---|
| bacLj-f | GATTGGGTATCATCGTTGGG |
| acman_7520d | GGATCAAGAGCTACCAACTG?? |
| acman_8363u | CGCTGACTTTGAGTGGAATG |
| bacRend-f | CTCCTCGTTCTCCCTGCACATG |
| acman7929-f | gtgtaaaacgacggccagtg |
| acman8261-r | gttcaatgatatccagtgcag |

**E. Primers used for positioning attachment sites (attB) at a) nbs locus and b) Ilp locus**

**a) attB at nbs**

| **primer name** | **sequence** |
|---|---|
| nbsGalk-f | ggctgatggtatggtaacctgtgtttaatgtcgtgcctaaacgtaattaaCCTGTTGACAATTAATCATCGGCA |
| nbsGalk-r | tatttcgcaagtttattgttagcaaaataaagtaactttacaagcgacggTCAGCACTGTCCTGCTCCTT |
| nbs2776-f | ccaggaaactgaatcctcct |
| nbs3169-r | cggccgcaagaactttaaga |

**b) attB at Ilp**

| | |
|---|---|
| bac810Galk_f | cacaatgaaatgatactaacgatacttaaaaacgtgttcaaactcttgtcaatattgtaaaaaacctgttgacaattaatcatcggca |
| bac810Galk_r | caaatggtcatctgaccaaattcctaaatgaaagagaatgttgtttgccttttttgaatatcagcactgtcctgctcctt |
| bac810_att-end | cacaatgaaatgatactaacgatacttaaaaacgtgttcaaactcttgtcaatattgtaaaaaaatcgataccgtcgacatgcc |
| bac810_att-head | caaatggtcatctgaccaaattcctaaatgaaagagaatgttgtttgccttttttgaatattcgacgatgtaggtcacggt |

**F. Primers used for a) removing I-SceI at IS1 and b) placing a new one at IS2**

**a) removing I-SceI at IS1**

| **primer name** | **sequence** |
|---|---|
| up7993Galk-f | ccagtgagcgcgcgtaatacgactcactatagggcgaattggagctcgttt **cctgttgacaattaatcatcggca** |
| dn7993Galk-r | gaccgctcgaggtttcctgcaggcgtacgcgtgcatgctagcggatcc **tcagcactgtcctgctcctt** |
| acman7929-f | gtgtaaaacgacggccagtg |
| acman8029-r | gccggcgcgccatcgataac |

**a) placing I-SceI at IS2**

| **primer name** | **sequence** |
|---|---|
| up8150Galk-f | GCGATAGAATGAGTGCGAGGCCGAGATAGTCGAGATAGCCGAGATACAATAC **cctgttgacaattaatcatcggca** |
| dn8150Galk-r | ctactttccgcaaaaatgggttttattaacttacatacatactagaattc **tcagcactgtcctgctcctt** |
| up8150IS2-f | GCGATAGAATGAGTGCGAGGCCGAGATAGTCGAGATAGCCGAGATACAATAC**ATTACCCTGTTATCCCTA** |

| | |
|---|---|
| dn8150IS2-r | ctactttccgcaaaaatgggttttattaacttacatacatactagaattc **TAGGGATAACAGGGTAAT** |
| up8150IS2plus-f | *CTAGATATCGCCCGATTCAGATGCGGATATGGGAATGTG***GCGATAGAATGAGTGCGAGG** |
| dn8150IS2plus-r | ctactttccgcaaaaatggg |

**G. Primers used for attachment site PCR assay**

| **primer name** | **sequence** |
|---|---|
| nbs2858 | caatcgcaagttgtccaagg |
| nbs3169 | cggccgcaagaactttaaga |
| bac810L-f | cgataatcgaatgcactgaag |
| bac810R-r | ccagtcactgcaatcgtag |